



Original Research

Identification of tau-tubulin kinase 1 inhibitors by microfluidics-based mobility shift assay from a kinase inhibitor library

Jinlei Wang^{a,b}, Ying Lin^a, Xiaoyu Xu^b, Yonghui Wang^{a,*}, Qiong Xie^{a,*}

^a School of Pharmacy, Fudan University, 826 Zhangheng Road, Shanghai 201203, PR China

^b Shanghai ChemPartner Co. Ltd., 2727/2728 Jinke Road, Shanghai 201203, PR China

ARTICLE INFO

Keywords:

Alzheimer's disease (AD)
tau tubulin kinase 1 (TTBK1)
microfluidics-based mobility shift assay (MMSA)
Molecular docking

ABSTRACT

Tau tubulin kinase 1 (TTBK1) is a serine/threonine/tyrosine kinase that phosphorylates multiple residues in tau protein. Hyperphosphorylated tau is the main cause of tauopathy, such as Alzheimer's disease (AD). Therefore, preventing tau phosphorylation by inhibiting TTBK1 has been proposed as a therapeutic strategy for AD. However, few substrates of TTBK1 are reported for a biochemical assay and few inhibitors targeting TTBK1 have been reported so far. In this study, we identified a fluorescein amidite (FAM)-labeled peptide 15 from a small peptide library as the optimal peptide substrate for human TTBK1 (hTTBK1). We then developed and validated a microfluidics-based mobility shift assay (MMSA) with peptide 15. We further confirmed that peptide 15 could also be used in the ADP-Glo kinase assay. The established MMSA was applied for screening of a 427-compound kinase inhibitor library, yielding five compounds with IC₅₀s of several micro molar against hTTBK1. Among them, three compounds, AZD5363, A-674,563 and GSK690693 inhibited hTTBK1 in an ATP competitive manner and molecular docking simulations revealed that they enter the ATP pocket and form one or two hydrogen bonds to the hinge region with hTTBK1. Another hit compound, piceatannol, showed non-ATP competitive inhibitory effect on hTTBK1 and may serve as a starting point to develop highly selective hTTBK1 inhibitors. Altogether, this study provided a new *in vitro* platform for the development of novel hTTBK1 inhibitors that might have potential applications in AD prevention.

Introduction

Protein kinases are key regulators governing numerous biological processes, especially the regulation of cell signaling pathways and are appealing targets for drug discovery [5,19]. So far more than 60 FDA-approved therapeutic agents target protein kinases [30], but none of them for neurodegenerative diseases (<http://www.brimr.org/PKI/PKIs.htm>).

Tau tubulin kinase (TTBK) belongs to the casein kinase 1 (CK-1) super family having two isoforms: TTBK1 and TTBK2. TTBK1 is a serine/threonine/tyrosine kinase that is specifically expressed in the central nervous system (CNS) [6,22,32], and TTBK2 is widely distributed not only in brain but also in liver, heart, brain, etc. [15]. TTBK1 was first characterized in 2006 to be responsible for tau phosphorylation and aggregation [32]. Hyperphosphorylated tau, which aggregates in the forms of paired helical filaments (PHFs) and neurofibrillary tangles (NFTs), is implicated in the pathogenesis of Alzheimer's disease (AD) [1,21,23,36]. Moreover, recent evidence shows that TTBK1 phosphorylates tau at specific sites that match PHF-specific

phosphorylation sites (Y197, S198, S199, S202 and S422) [32]. It was reported that a potent TTBK1 inhibitor could lower Tau phosphorylation *in vivo* [12] and the upregulation of TTBK1 has been linked to AD pathology in human [33]. Thus, TTBK1 is a promising drug target for AD [2].

The first two TTBK1 inhibitors were reported in 2013, namely 3-[(6,7-dimethoxyquinazolin-4-yl)amino]phenol (compound 1, Fig. 1) and methyl 2-bromo-5-(7H-pyrrolo[2,3-d]pyrimidin-4-ylamino)benzoate (compound 2, Fig. 1), which were validated by surface plasmon resonance (SPR) binding assays [37]. Compound 1, also named WHI-P180, was used as the reference compound in this study. Compound 2 is related to a reported Akt inhibitor [20]. The reported dissociation constants of both compounds on phosphorylated TTBK1 were 0.46 μ M and 30 μ M, respectively [37]. The third inhibitor is 3-[(5-[(4-amino-4-methylpiperidin-1-yl)methyl]pyrrolo[2,1-f][1,2,4]triazin-4-yl)amino]-5-bromophenol (compound 3, Fig. 1) that inhibits TTBK1 and TTBK2 with IC₅₀s of 120 nM and 170 nM, respectively [18]. However, for these three inhibitors, no more data regarding their further development is reported up to now.

* Correspondence.

E-mail addresses: yonghuiwang@fudan.edu.cn (Y. Wang), qxie@fudan.edu.cn (Q. Xie).

<https://doi.org/10.1016/j.slasd.2023.06.003>

Received 3 April 2023; Received in revised form 22 May 2023; Accepted 27 June 2023

Available online 1 July 2023

2472-5552/© 2023 The Authors. Published by Elsevier Inc. on behalf of Society for Laboratory Automation and Screening. This is an open access article under the CC BY-NC-ND license (<http://creativecommons.org/licenses/by-nc-nd/4.0/>)

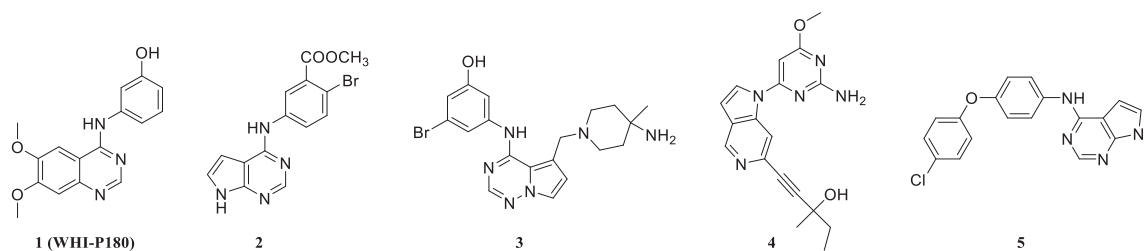


Fig. 1. Structures of TTBK1 inhibitors (compounds 1, 2, 3, 4 and 5).

In 2021, Tamara Halkina et al. identified a potent TTBK1 inhibitor compound 4 (cell IC_{50} : 315 nM, Fig. 1) using an antibody-based time-resolved fluorescence energy transfer (TR-FRET) assay, which inhibits tau phosphorylation at the disease-related S422 site *in vivo* models [12]. And most recently, another compound 5 (biochemical IC_{50} : 240 nM, Fig. 1) was reported with more than 17 folds of selectivity against TTBK2 [26].

Besides the aforementioned TTBK1 inhibitors, there were scarcely few inhibitors described for TTBK1 up to now. And TTBK2 is also attributed to tau phosphorylation on residues of Ser208 and Ser210, which are characteristics of the PHF phosphorylation in brain [11]. Hence, additional potent TTBK1 inhibitors, especially those with different structures, inhibition mechanisms and high selectivity on TTBK1, are urgently needed.

Although various methods, such as TR-FRET, ADP-Glo kinase assay, and [γ - ^{32}P] ATP-based isotope assay [10] are used for kinase activity studies, few regarding hTTBK1 were reported due to no published peptide substrate commonly used in biochemical assays. Therefore, substrate selection is a key step to establish a TTBK1 biochemical assay. SPR method has low throughput and TR-FRET assay cannot be used in continuous manner. Thus, an HTS-friendly and continuous method, microfluidics-based mobility shift assay (MMSA), is developed, which includes two systems, the on-chip electrophoretic separation system and the quantification system. Through these two systems, the fluorescence-labeled substrate and product will be separated due to the changes in charge and/or mass as a result of phosphorylation and amounts quantified by fluorescence intensities [13]. In this way, the potential fluorescence interference from testing compounds will be minimized because of the direct readout of substrate conversion. Moreover, the capability of monitoring enzymatic progress in real time makes it feasible to perform kinetic study. In this study, a microfluidics-based mobility shift assay (MMSA) was developed for TTBK1 with the fluorescein amidite (FAM)-labeled peptide 15, and validated by compound 1 (WHI-P180). The assay has been applied for screening of a 427-compound kinase inhibitor library, yielding some hits with IC_{50} s of several micro molar against hTTBK1.

Materials and methods

Reagents

The Fluorescein amidite (FAM)-labeled peptide substrates for MMSA were synthesized by GL Biochem (Shanghai, China). The 384 well plates (Corning, cat#3575) were from Corning (New York, USA). hTTBK2 were purchased from Carna Bioscience (cat# 03–109). ADP-Glo kinase assay kit was purchased from Promega (cat# V9102). The ProxiPlate-384 plates were purchased from PerkinElmer (Waltham, USA). LANCE Ultra ULIGHT™-DNA Topoisomerase 2- α -Thr1342 Peptide and LANCE Ultra Europium-anti-phospho-DNA Topoisomerase 2- α -Thr1342 were purchased from PerkinElmer (Waltham, USA). The 427 compounds are from a kinase inhibitor library (Selleck, Cat# L1200), and all of them are validated protein kinase inhibitors. All compounds were stored as 10 mM stock in DMSO. TTBK1-IN-1 (compound 4) was purchased from

MedChemExpress (MCE, cat# HY-134,968). All other reagents were purchased from Sigma Aldrich (St. Louis, USA).

Instrumentation

The MMSA was carried out at room temperature using a LabChip EZ Reader II system from PerkinElmer (Waltham, USA) equipped with a 12-sipper chip in separation buffer. The reaction samples were sipped by a 12-sipper chip, and then the fluorescent product and substrate were separated under a screen pressure of -1.2 psi. In the step of detection, the fluorescent analytes were stimulated by a blue LED (450–490 nm) and detected by a CCD camera (515–550 nm).

The separation of peptide 15 was performed with the optimized conditions: upstream voltage = -500 V, downstream voltage = -2250 V, a screen pressure = -1.2 psi, base pressure = -0.5 psi. The separation buffer contained 100 mM HEPES, 1 mM EDTA, 0.015% Brij-35, 5% DMSO and 0.2% coating-3 reagent (PerkinElmer, Waltham, USA), pH 7.5. The substrate conversion rate was defined as the peak height of product divided by the sum of both substrate and product.

Construct cloning

The coding sequence of human tau tubulin kinase 1 catalytic domain (residue 1–343, accession number: NP_115,927.1) was cloned into pFastBac1 vector (Thermo Fisher, USA) with an N-terminal GST-tag by the 5' *Bam*HI site and the *Xho*I site at the 3' end after a TGA stop codon. The fidelity of this construct was verified by DNA sequencing.

Expression and purification

The constructed vector was transformed into DH10Bac E. coli competent cells, and the baculovirus was generated from the pFastBac clones for insect-cell expression following standard procedures. For protein production, Sf9 insect cells were infected with baculovirus for 66 h at a 1:100 virus:cell ratio (volume ratio of virus to sf9 cells). The infected cells were harvested by centrifuge at 200 g for 10 min and the cell pellets were stored in liquid nitrogen.

The cell pellets were resuspended and sonicated in buffer A (20 mM Tris-HCl buffer pH8.0 containing 5 mM $MgCl_2$, 300 mM NaCl, 5% glycerol, 0.05% CHAPS and 1 mM DTT) and centrifuged at 40,000 g for 30 min. The recombinant protein was purified from the supernatant with Glutathione Sepharose 4B affinity-chromatography column (GE Healthcare), dialyzed against buffer A, and was further purified with HiTrap Q HP column equilibrated by buffer A, and concentrated to 2 mg/mL in 20 mM Tris-HCl pH 7.5 containing 5 mM $MgCl_2$, 150 mM NaCl, 1 mM DTT and 10% glycerol.

hTTBK1 inhibition study with microfluidics-based mobility shift assay

hTTBK1 activity was measured continuously with the microfluidics-based mobility shift assay in reaction buffer (20 mM HEPES, pH 7.5, 10 mM $MgCl_2$, 0.01% TritonX-100 and 0.01% BSA). Briefly, 3 nM of hTTBK1 proteins were added to 384 well plates, which was pre-dispensed

with 100 nL of compounds or DMSO by Echo550 system (Labcyte, San Jose, USA). After 15 min pre-incubation at 25 °C of hTTBK1 and compounds or DMSO, 80 μM of ATP and 1 μM of peptide 15 were added to start the enzymatic reaction. After incubation at 25 °C for 2.5 h, the reactions were terminated by adding 25 μL stop buffer (200 mM HEPES, pH 7.5, 2 mM EDTA, 0.03% Brij-35, 0.4% coating-3 reagent) to each well. For negative control wells, 1 × reaction buffer alone was added instead of hTTBK1. The hTTBK2 inhibition study with MMSA is the same as hTTBK1. The percentage of inhibition was calculated as $\frac{(S_{\text{positive}} - S_{\text{sample}})}{(S_{\text{positive}} - S_{\text{negative}})}$, and the dose-response curve of hTTBK1 inhibitors were fitted to equation 1 to generate the IC₅₀ values:

$$Y = \text{Bottom} + \frac{(\text{Top} - \text{Bottom})}{(1 + 10^{((\text{LogIC}_{50} - X) \times \text{HillSlope}))}} \quad (1)$$

Where Y is the percentage of inhibition, Top and Bottom represent the signal of positive and the signal of negative, respectively, and X is molar concentration of compound.

Pilot screening with the kinase inhibitor library

Kinase inhibitor library containing 427 compounds were screened against hTTBK1 for their activities at 10 μM. Assays were performed in reaction buffer (20 mM HEPES, pH 7.5, 10 mM MgCl₂, 0.01% TritonX-100 and 0.01% BSA) in 384-well plates. The enzymatic reactions were initiated by the addition of ATP (80 μM) and peptide 15 (1 μM) to a reaction mixture containing 3 nM of hTTBK1 and pre-dispensed compounds or DMSO. After incubation at 25 °C for 2.5 h (at endpoint), the reactions were terminated by adding 25 μL stop buffer (200 mM HEPES, pH 7.5, 2 mM EDTA, 0.03% Brij-35, 0.4% coating-3 reagent) to each well. For negative control wells, 1 × reaction buffer alone was added instead of hTTBK1.

For dose-response test, the selected compounds were screened against hTTBK1 and hTTBK2 with dose from 0.2 μM to 200 μM, and other conditions were the same as above. Z' factor was calculated to evaluate the assay quality using the following equation 2:

$$z' = 1 - 3 \times \frac{(\text{SD of negative} + \text{SD of positive})}{(\text{mean of positive} - \text{mean of negative})} \quad (2)$$

Mechanism of action (MOA) study

Varied concentrations of compound were dispensed into 384-well plates, and then 3 nM of hTTBK1 were added into each well. After 15 min pre-incubation at 25 °C of hTTBK1 and compounds or DMSO, serially diluted ATP and 1 μM of peptide 15 were added to start the enzymatic reaction. Enzymatic activity was measured after 2.5 h reaction with microfluidics-based mobility shift assay. To generate K_m and V_{max} values, the calculated rate of product formation and ATP concentration were fitted to Michaelis-Menten equation 3:

$$Y = V_{\text{max}} \times \frac{X}{K_m + X} \quad (3)$$

All the above equations can be referred to the book [4].

TTBK1 inhibition study with ADP-Glo assay

In parallel, a homogeneous ADP-Glo assay was developed with 384-well format to measure hTTBK1 activity. The enzymatic reactions were performed the same way as described above for MMSA, except that the reactions were stopped by adding 5 μL of ADP-Glo reagent to each well, incubate at 25 °C for 1.5 h, and then add 10 μL of kinase detection reagent to detect ADP production. The percentage of inhibition and the IC₅₀ values were calculated as previous described.

TTBK1 inhibition study with TR-FRET assay

The inhibitory activity of WHI-P180 was tested with TR-FRET assay, as developed by Tamara Halkina et al. [12] with minor modifications. In brief, 1 nM of hTTBK1 and 200 nM LANCE Ultra ULIGHT™-DNA Topoisomerase 2-α-Thr1342 Peptide (Perkin Elmer) were added to 384-well plates pre-dispensed with 100 nL of compound or DMSO. 80 μM of ATP was added to start the enzymatic reactions. After 150 min of incubation at 25 °C, quenching and detection solution containing LANCE Ultra Europium-anti-phospho-DNA Topoisomerase 2-α-Thr1342 (Perkin Elmer) and 80 mM EDTA was added to terminate the enzymatic reactions, and plates read with Envision (320 nm for excitation, 615 nm for emission, 665 nm for 2nd emission). The percentage of inhibition and the IC₅₀ values were calculated as previous described.

Molecular docking study

Molecular docking was carried out using the Maestro 12.9.123 software package. The co-crystal structures of TTBK1 (PDB: 4BTM, resolution of 2.54 Å) [37] were selected and processed by the Protein Preparation Wizard including water deletion, addition of missing hydrogen atoms, and adjustment of the tautomerization and protonation states of histidine. The protein was subjected to Monte Carlo multiple minimum conformational searches using the OPLS4 force field. The docking grid was centered according to the ligand position. Other parameters were set as default. This docking was performed with Glide-docking using the Standard Precision (GlideSP) algorithm. The final ranking from the docking was based on the docking score, and high scoring complexes were inspected visually to select the most reasonable solution.

Results and discussion

Peptide selection for MMSA

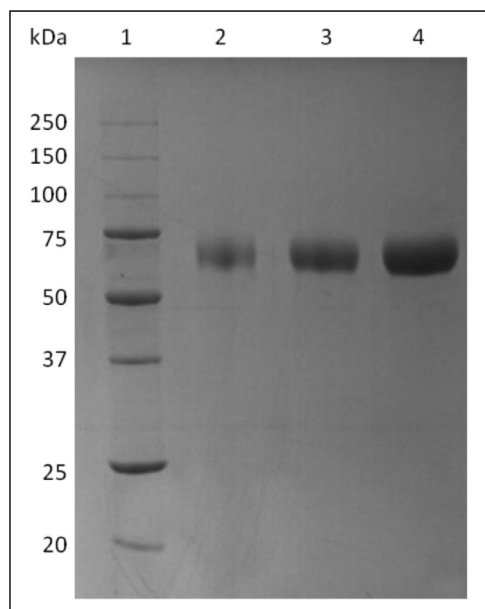
We purified hTTBK1 using the baculovirus expression system and the protein purity was above 85% as determined by Coomassie Brilliant Blue staining on SDS-PAGE (Fig. 2). We then screened a small peptide library (our internal peptide library for MMSA, Table S1) and identified peptide 15 (5'-FAM-KKLNRRLSVA-COOH) as the optimal substrate for hTTBK1. Peptide 3, peptide 15 and peptide 16 with highest conversion rates were selected to perform kinetic study to calculate their specific activities. The specific activity of hTTBK1 measured at 1 μM peptide 15 and 20 nM hTTBK1 was 1.08 μmol/min/mg (Table 1), much higher than other peptides except peptide 16 (5'-FAM-KKLNRRLSVA-COOH). Although peptide 16 had higher enzymatic rate, it has lower signal to noise (S/B) than peptide 15 (16.3 vs. 14, Table 1). Besides, the topoisomerase II peptide used in the TR-FRET assay, FAM-labeled DNA Topoisomerase 2-α-Thr1342 Peptide (5'-FAM-DEKTDDE-COOH), was synthesized by GL Biochem and its conversion rate was detected at 20 nM of hTTBK1. However, the conversion rate of DNA Topoisomerase 2-α-Thr1342 Peptide was lower than that of peptide 15 (9.57% vs. 15.01%) (Table 1). Therefore, peptide 15 was selected for hTTBK1 biochemical assay development.

Michale Bouskila et al. reported a peptide substrate for TTBK2 (isotope assay) [3]. However, there has been no published peptide substrate optimal for hTTBK1 biochemical assay so far. Peptide 15 identified here might be the first validated hTTBK1 peptide substrate as tested with known inhibitors.

We also applied peptide 15 to a bioluminescence-based ADP-Glo kinase assay and further confirmed with the serially diluted WHI-P180 to obtain a similar IC₅₀ to that generated by MMSA (details described in the part of "MMSA optimization and validation"). Therefore, peptide 15 (5'-FAM-KKLNRRLSVA-COOH) could be used as the substrate of hTTBK1 in biochemical assays including MMSA and ADP-Glo assay.

Table 1
Peptide selection for MMSA.

Peptide	Conversion (%) ^a		S/B	Rate ($\mu\text{mol}/\text{min}$ per mg)
	20 nM hTTBK1	reaction buffer		
Peptide 1	5.41 \pm 1.62	0.82 \pm 0.02	6.6	ND
Peptide 2	7.93 \pm 0.26	0.85 \pm 0.06	9.3	ND
Peptide 3	9.25 \pm 0.29	0.78 \pm 0.02	11.8	0.78
Peptide 4	2.71 \pm 0.06	0.75 \pm 0.04	3.6	ND
Peptide 5	5.05 \pm 0.14	0.79 \pm 0.05	6.4	ND
Peptide 6	5.47 \pm 0.26	0.69 \pm 0.12	8.0	ND
Peptide 7	7.12 \pm 0.14	0.85 \pm 0.05	8.3	ND
Peptide 8	6.00 \pm 0.25	0.73 \pm 0.01	8.3	ND
Peptide 9	4.91 \pm 0.13	0.83 \pm 0.04	5.9	ND
Peptide 10	2.28 \pm 0.05	0.92 \pm 0.05	2.5	ND
Peptide 11	4.84 \pm 0.02	0.91 \pm 0.06	5.3	ND
Peptide 12	5.20 \pm 0.07	0.67 \pm 0.05	7.7	ND
Peptide 13	6.66 \pm 1.20	0.78 \pm 0.02	8.6	ND
Peptide 14	5.60 \pm 0.30	0.87 \pm 0.01	6.5	ND
Peptide 15	15.01 \pm 0.49	0.92 \pm 0.03	16.3	1.08
Peptide 16	17.54 \pm 0.03	1.26 \pm 0.04	14.0	1.28
Peptide 17	4.64 \pm 0.18	0.85 \pm 0.02	5.5	ND
Peptide 18	4.79 \pm 0.19	0.70 \pm 0.03	6.8	ND
Peptide 19	6.43 \pm 1.93	0.83 \pm 0.05	7.7	ND
Peptide 20	8.15 \pm 0.39	0.83 \pm 0.04	9.8	ND
Peptide 21	3.84 \pm 0.18	1.44 \pm 0.09	2.7	ND
Peptide 22	2.06 \pm 0.07	0.78 \pm 0.13	2.7	ND
Peptide 23	5.24 \pm 0.23	0.74 \pm 0.01	7.1	ND
Peptide 24	5.24 \pm 0.14	0.69 \pm 0.06	7.6	ND
Peptide 25	5.24 \pm 0.12	0.69 \pm 0.07	7.6	ND
DNA Topoisomerase	9.57 \pm 0.30	1.59 \pm 0.11	6.0	ND
2-alpha-Thr1342 Peptide				

^a . All the results represent the arithmetic mean value \pm standard deviation of duplicate data.**Fig. 2.** SDS-PAGE analysis of hTTBK1 (1–343) purified using baculovirus expression system. The samples were electrophoresed on a 4–12% Bis-Tris Nu-PAGE gel (Invitrogen) and stained with Coomassie Brilliant Blue. Lane 1, molecular-weight marker (kDa); lane 2, 0.5 μg of hTTBK1 (1–343); lane 3, 1 μg of hTTBK1 (1–343); lane 4, 2 μg of hTTBK1 (1–343).

MMSA optimization and validation

It was reported that millimolar levels of Mg^{2+} ions were essential for hTTBK1 kinase activity [32], so we titrated Mg^{2+} firstly (Fig. S1) and finally MgCl_2 was added at 10 mM in the basic kinase buffer (20 mM HEPES, pH 7.5, 0.01% TritonX-100 and 0.01% BSA) as the final reaction buffer for hTTBK1. A linear dose-response was exhibited when hTTBK1

was titrated in the range of 0.78–12.5 nM with the selected substrate peptide 15 ($r^2 = 0.9965$, Fig. 3A). In the kinetic reading mode, the enzymatic reaction progression curves were linear for 3 h when the concentrations of hTTBK1 were 6.25 nM and 3.13 nM (Fig. 3B). The data showed that several nanomolar of hTTBK1 can be used in MMSA that nanomolar inhibitors can be characterized. The ATP conversion rate and ATP concentrations were fitted to Michaelis–Menten equation (equation 3) and the K_m of ATP was calculated as 13.7 μM (Fig. 3C). Therefore, 15 μM of ATP were used for the subsequent kinase inhibitor screening.

As to robustness, the MMSA with Z' factor of 0.83 and assay window of 8.7 (ratio of signal to background) was considered excellent for compound screening (Fig. 3D). DMSO tolerance was also studied and no significant effect was observed with up to 4% DMSO in enzyme reaction system (data not shown).

WHI-P180 (compound 1, Figs. 1 and 3E), an anilinoquinazolines family compound, is a multi-kinase inhibitor with IC_{50} s of 4.5 nM, 66 nM and 4 μM on RET, KDR and EGFR, respectively [9,25]. It was reported that WHI-P180 could bind with K_d s of 0.46 μM and 0.24 μM for phosphorylated and nonphosphorylated TTBK1 calculated by surface plasmon resonance (SPR) [37]. Fig. 3F shows the IC_{50} value of 3.3 μM for WHI-P180 to inhibit TTBK1 with our optimized MMSA described above, which is in agreement with the recent data showing that WHI-P180 can inhibit TTBK1 with IC_{50} of 4.61 μM [12]. Besides, three different methods, MMSA, ADP-Glo and TR-FRET, generate IC_{50} s with no more than 3 folds variance, which indicates that the peptide 15 could be used for the subsequent compound screening. In order to make further validation for compound screening, IC_{50} of TTBK1-IN-1 (compound 4) was also tested with MMSA (6.3 nM, Fig S2), which was slightly less potent than the activity reported in the literature (2.7 nM) [12].

Staurosporine, a pan kinase inhibitor that inhibits most protein kinases through interfering with ATP binding [24,31,34], shows no inhibitory effect on hTTBK1 activity at concentration up to 200 μM (Fig. S2). The result of staurosporine was surprising given the structural similarity between TTBK1 and other protein kinases [18,27]. But in another literature, it was reported that staurosporine did not bind to TTBK1 in a crystal structure study with TTBK1 and staurosporine, which was further

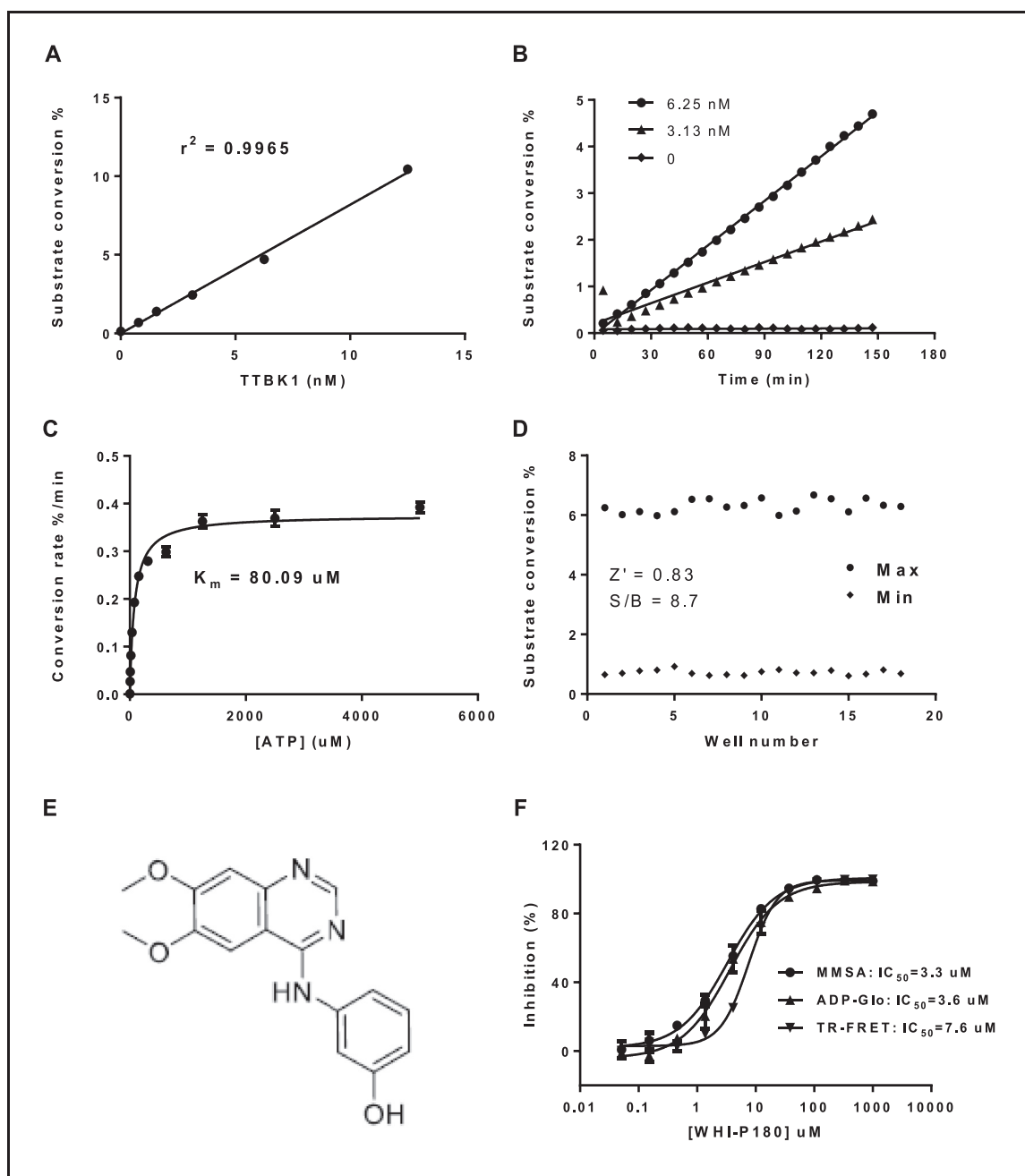


Fig. 3. hTTBK1 MMSA optimization and validation.

A. Titration of hTTBK1 in the assay, 40 μM of ATP; **B.** Time course of hTTBK1 enzyme reaction, 40 μM of ATP; **C.** Michaelis-Menten plot for ATP, 10 nM of hTTBK1, data were performed in duplicate; **D.** Performance of MMSA, Z' was calculated by equation 2 described above, S/B represents signal to background ratio, 5 nM of hTTBK1, 80 μM of ATP and 2.5 h reaction time; **E.** The structure of WHI-P180; **F.** Dose-response curve for WHI-P180 inhibition on hTTBK1 with MMSA, ADP-Glo and TR-FRET assays, data were performed in duplicate.

confirmed by TTBK1 activity assay and fluorescent dye-binding thermal stability assay [18].

Pilot screening of kinase inhibitor library with MMSA

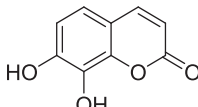
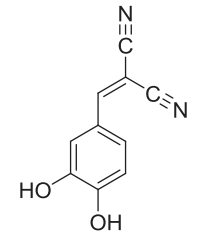
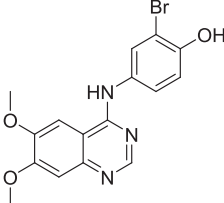
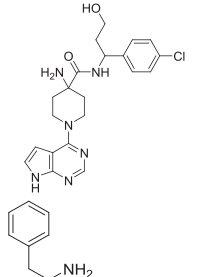
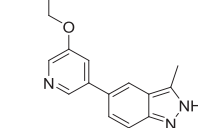
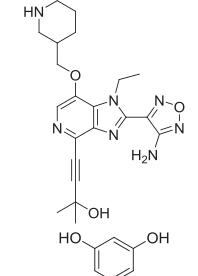
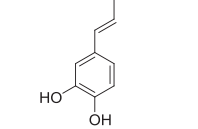
A pilot screening of a kinase inhibitor library, with 427 known kinase inhibitors including 34 FDA approved ones [30], was performed against hTTBK1 with optimized MMSA, and the pilot screening results of all the 427 inhibitors were listed in Table S2. A Z' factor above 0.6 (Table S3) was yielded from each plate, confirming the assay quality remained high throughout this pilot screen. 7 compounds showed inhibition above 40% at 10 μM on hTTBK1 (Table 2), which were further studied for their

dose-response characteristics against both hTTBK1 and hTTBK2, and the fitted IC_{50} s calculated by equation 1 were listed in Table 2 and all the dose-response curves were listed in Supplementary Information (Fig. S4 and S5).

Both daphnetin and AG-18 were EGFR inhibitors with IC_{50} s of 7.67 μM and 35 μM , respectively [8,38], and they showed very weak inhibitory effect on hTTBK1 and hTTBK2 with IC_{50} s of more than 25 μM (Table 2). The structure of WHI-P154 is similar to WHI-P180 except for a 3-bromo-4-hydroxyl substitution on the phenyl ring, and it is not surprising that WHI-P154 showed IC_{50} of 9.17 μM on hTTBK1, close to that of WHI-P180. And WHI-P154 showed inhibition with IC_{50} of 26.03 μM on hTTBK2.

Table 2

Biochemical characterization of 7 compounds selected from a 427-compound kinase inhibitor library.

Compound	hTTBK1		hTTBK2	Structure	MOA on hTTBK1	Targets
	Inhibition at 10 μ M (%) ^a	IC ₅₀ (μ M) ^a	IC ₅₀ (μ M) ^a			
daphnetin	54.01	22.44	36.56		ND	EGFR, PKA, PKC
AG-18	43.92	29.6	42.8		ND	EGFR
WHI-P154	47.29	9.17	26.03		ND	EGFR, JAK3
AZD5363	58.92	6.92	11.34		Competitive with ATP	AKT1/2/3
A-674,563	65.98	5.8	3.94		Competitive with ATP	AKT1
GSK690693	48.32	5.28	1.18		Competitive with ATP	AKT1/2/3
piceatannol	83.06	5.212	30.9		Non-competitive with ATP	Syk

^a All the results represent the arithmetic mean of duplicate data.

Other three hTTBK1 inhibitors yielded in this pilot screening, namely AZD5363, A-674,563 and GSK690693, showed inhibitory effect on hTTBK1 (Table 2) in an ATP competitive manner, with the same V_{\max} values and altered K_m (Fig. 4A-F) at different inhibitor concentrations.

AZD5363, A-674,563 and GSK690693 were docked into the TTBK1 protein binding site by Maestro 12.9.123 software package. The co-

crystal structure of TTBK1 with compound 2 (PDB: 4BTM, resolution of 2.54 Å) [37] was selected as the docking protein. From the docking results, these three compounds enter the ATP pocket (Fig. 5A), and form similar binding modes to compound 2, which explains that they are ATP-competitive inhibitors. Besides, A-674,563 and GSK690693 form two hydrogen bonds to the hinge region of hTTBK1 (Gln134), while AZD5363 forms one hydrogen bond with Gln134 (Fig. 5B-D), which

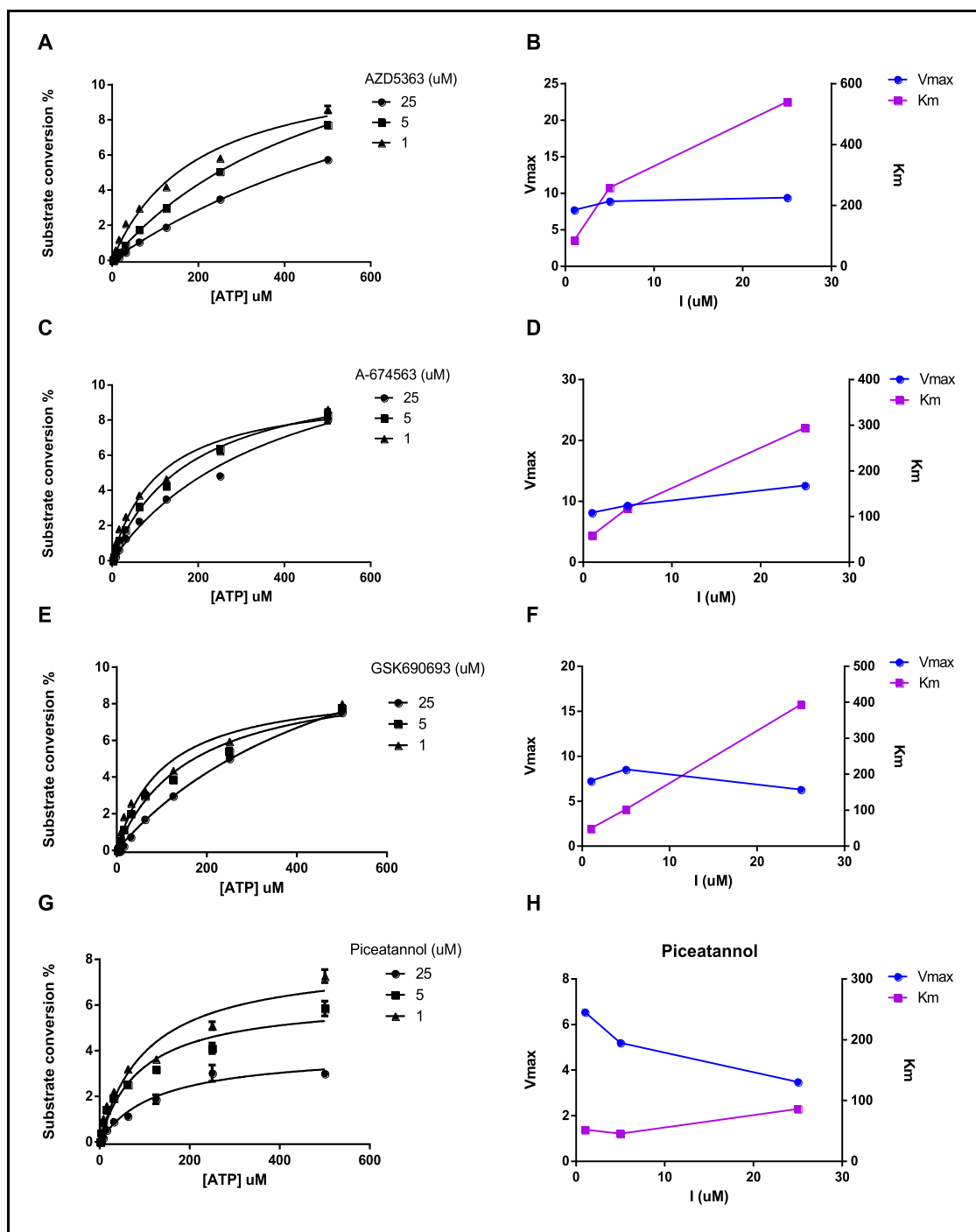


Fig. 4. MOA study of AZD5363 (A, B), A-674,563 (C, D), GSK690693 (E, F) and piceatannol (G, H). All the above data were performed in duplicate.

may explain the lower IC_{50} of A-674,563 and GSK690693 than that of AZD5363 (Table 2).

Piceatannol is a naturally occurring polyphenolic stilbenes that has previously been identified as Syk selective inhibitor [28]. It can also inhibit PKA, PKC, MLCK and CDPK in a dose-dependent manner with IC_{50} s of 3 μ M, 8 μ M, 12 μ M and 19 μ M [35]. In the present study, we firstly demonstrated that piceatannol exerted significant inhibitory effect against hTTBK1 and hTTBK2 in a dose-dependent manner (Table 2, IC_{50} s: 5.2 μ M vs. 30.9 μ M). The MOA study showed that piceatannol was a non-ATP competitive inhibitor (Fig. 4G-H), which indicated that piceatannol could prevent ATP from binding with hTTBK1.

It was reported that the kinase domains of hTTBK1 and hTTBK2 share 87.5% of identity and 96% of similarity [16,27], which poses a great challenge to develop selective hTTBK1 inhibitors in the ATP competitive manner. Piceatannol, identified in our screen as a non-ATP competitive hTTBK1 inhibitor, can serve as a hit compound to further design inhibitors specifically selective for hTTBK1.

Piceatannol has many biological activities like anticancer, antioxidant and anti-inflammatory effects [17,29], and possesses high potential to prevent Alzheimer's disease [7,14]. Since hTTBK1 has been linked to AD pathology in human [33], it is possible to speculate that piceatannol can inhibit hTTBK1 to decrease the level of phospho-tau and exert

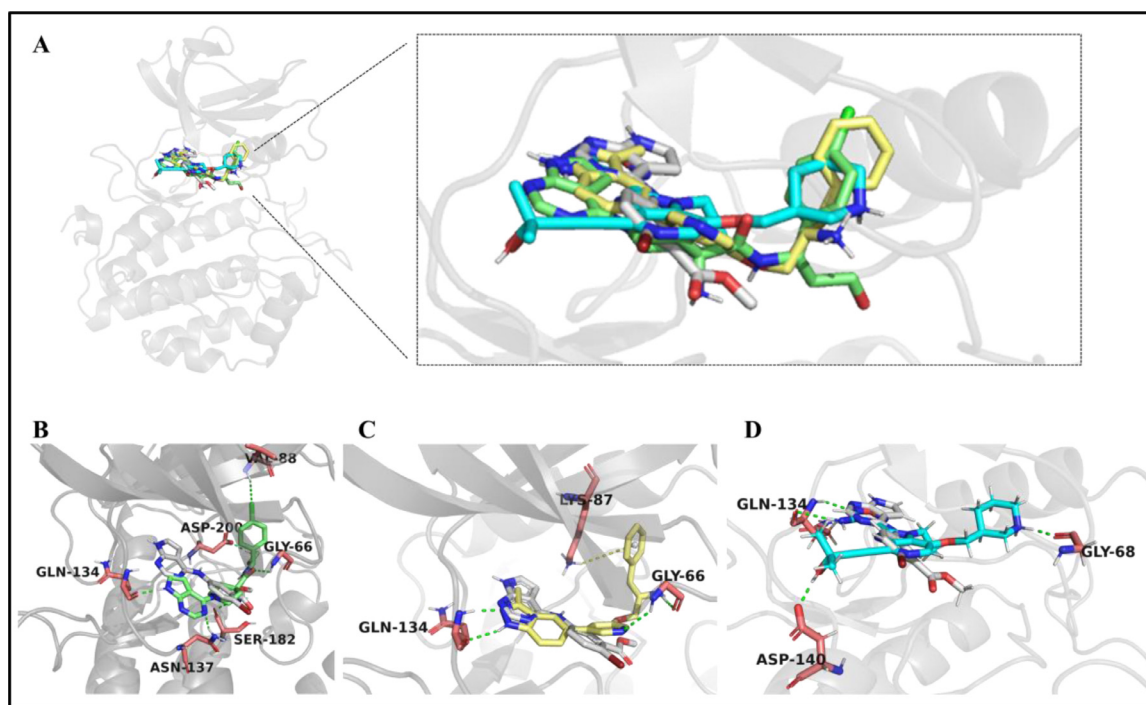


Fig. 5. Binding modes of AZD5363, A-674,563 and GSK690693 with TTBK1 (PDB code: 4BTM).

A. Overlay of three compounds binding with TTBK1; B–D. Binding modes of AZD5363 (in green, B), A674563 (in yellow, C) and GSK690693 (in cyan, D) with TTBK1 compared with compound 2 (in white), respectively. All the hydrogen bonds were indicated with green dashed line.

its neuroprotective effect. The true underlying mechanism needs to be further explored through *in vitro* and *in vivo* assays. The MMSA assay established in our study can be applied to develop selective hTTBK1 inhibitors as tool compounds for studies to explore the relationship between hTTBK1, tau-phosphorylation and AD pathogenesis.

Conclusion

In this study, a microfluidics-based mobility shift assay was developed and validated by testing a small peptide library to identify the optimal kinase substrate, and then applied to screen for hTTBK1 inhibitors. By using this *in vitro* assay, seven compounds were identified from a commercial 427-compound kinase inhibitor library, of which AZD5363, A-674,563 and GSK690693 showed inhibitory effect on hTTBK1 in an ATP competitive manner and piceatannol in a non-ATP competitive manner. Thus, these compounds enlarged hTTBK1 inhibitor set and may serve as starting points to discover selective hTTBK1 inhibitors.

Declaration of Competing Interest

The authors declare that they have no known competing financial interests or personal relationships that could have appeared to influence the work reported in this paper.

Acknowledgements

This work was supported by National Natural Science Foundation of China (Grant Numbers: 81973163; 81874287).

Supplementary Data

Supplementary data related to this article can be found online at [doi:10.1016/j.slasd.2023.06.003](https://doi.org/10.1016/j.slasd.2023.06.003).

Reference

- [1] Ballatore C, Lee VM, Trojanowski JQ. Tau-mediated neurodegeneration in Alzheimer's disease and related disorders. *Nat Rev Neurosci* 2007;8(9):663–72.
- [2] Bao C, Bajrami B, Marcotte DJ, Chodaparambil JV, Kerns HM, Henderson J, et al. Mechanisms of regulation and diverse activities of tau-tubulin kinase (TTBK) isoforms. *Cell Mol Neurobiol* 2021;41(4):669–85.
- [3] Bouskila M, Esoof N, Gay L, Fang EH, Deak M, Begley MJ, et al. TTBK2 kinase substrate specificity and the impact of spinocerebellar-ataxia-causing mutations on expression, activity, localization and development. *Biochem J* 2011;437(1):157–67.
- [4] Copeland RA. *Enzymes: a practical introduction to structure, mechanism, and data analysis*. John Wiley & Sons; 2000.
- [5] Cui JJ. A new challenging and promising era of tyrosine kinase inhibitors. *ACS Med Chem Lett* 2014;5(4):272–4.
- [6] Dillon GM, Henderson JL, Bao C, Joyce JA, Calhoun M, Amaral B, et al. Acute inhibition of the CNS-specific kinase TTBK1 significantly lowers tau phosphorylation at several disease relevant sites. *PLoS ONE* 2020;15(4):e0228771.
- [7] Fu Z, Yang J, Wei Y, Li J. Effects of piceatannol and pterostilbene against β -amyloid-induced apoptosis on the PI3K/Akt/Bad signaling pathway in PC12 cells. *Food Funct* 2016;7(2):1014–23.
- [8] Gazit A, Yaish P, Gilon C, Levitzki A. Tyrosinostins I: synthesis and biological activity of protein tyrosine kinase inhibitors. *J Med Chem* 1989;32(10):2344–52.
- [9] Ghosh S, Jennissen JD, Liu XP, Uckun FM. 4-[3-Bromo-4-hydroxyphenyl]amino]-6,7-dimethoxyquinazolin-1-ium chloride methanol solvate and 4-[(3-hydroxyphenyl)amino]-6,7-dimethoxy-1-quinazolinium chloride. *Acta Crystallogr C* 2001;57(Pt 1):76–8.
- [10] Glickman JF, et al. *Assay Development for Protein Kinase Enzymes* Assay guidance manual. Markossian S, Grossman A, Brimacombe K, et al., editors. Eli Lilly & Company and the National Center for Advancing Translational Sciences; 2004. Bethesda (MD).
- [11] Goedert M, Spillantini MG, Jakes R, Rutherford D, Crowther RA. Multiple isoforms of human microtubule-associated protein tau: sequences and localization in neurofibrillary tangles of Alzheimer's disease. *Neuron* 1989;3(4):519–26.
- [12] Halkina T, Henderson JL, Lin EY, Himmelbauer MK, Jones JH, Nevalainen M, et al. Discovery of Potent and Brain-Penetrant Tau Tubulin Kinase 1 (TTBK1) Inhibitors that Lower Tau Phosphorylation In Vivo. *J Med Chem* 2021;64(9):6358–80.
- [13] Harrison DJ, Fluri K, Seiler K, Fan Z, Effenhauser CS, Manz A. Micromachining a miniaturized capillary electrophoresis-based chemical analysis system on a chip. *Science* 1993;261(5123):895–7.
- [14] Hassaan Y, Handoussa H, El-Khatib AH, Linscheid MW, El Sayed N, Ayoub N. Evaluation of plant phenolic metabolites as a source of Alzheimer's drug leads. *Biomed Res Int* 2014;2014:843263.
- [15] Houlden H, Johnson J, Gardner-Thorpe C, Lashley T, Hernandez D, Worth P, et al. Mutations in TTBK2, encoding a kinase implicated in tau phosphorylation, segregate with spinocerebellar ataxia type 11. *Nat Genet* 2007;39(12):1434–6.
- [16] Ikezu S, Ikezu T. Tau-tubulin kinase. *Front Mol Neurosci* 2014;7:33.

- [17] Kershaw J, Kim KH. The Therapeutic Potential of Piceatannol, a Natural Stilbene, in Metabolic diseases: a review. *J Med Food* 2017;20(5):427–38.
- [18] Kiefer SE, Chang CJ, Kimura SR, Gao M, Xie D, Zhang Y, et al. The structure of human tau-tubulin kinase 1 both in the apo form and in complex with an inhibitor. *Acta Crystallogr F Struct Biol Commun* 2014;70(Pt 2):173–81.
- [19] Lee PY, Yeoh Y, Low TY. A recent update on small-molecule kinase inhibitors for targeted cancer therapy and their therapeutic insights from mass spectrometry-based proteomic analysis. *Febs j* 2022.
- [20] Lippa B, Pan G, Corbett M, Li C, Kauffman GS, Pandit J, et al. Synthesis and structure based optimization of novel Akt inhibitors. *Bioorg Med Chem Lett* 2008;18(11):3359–63.
- [21] Luna-Viramontes NI, Campa-Córdoba BB, Ontiveros-Torres M, Harrington CR, Villanueva-Fierro I, Guadarrama-Ortíz P, et al. PHF-Core Tau as the potential initiating event for Tau Pathology in Alzheimer's disease. *Front Cell Neurosci* 2020;14:247.
- [22] Lund H, Cowburn RF, Gustafsson E, Strömberg K, Svensson A, Dahllund L, et al. Tau-tubulin kinase 1 expression, phosphorylation and co-localization with phospho-Ser422 tau in the Alzheimer's disease brain. *Brain Pathol* 2013;23(4):378–89.
- [23] Mandelkow E, von Bergen M, Biernat J, Mandelkow EM. Structural principles of tau and the paired helical filaments of Alzheimer's disease. *Brain Pathol* 2007;17(1):83–90.
- [24] Meggio F, Donella Deana A, Ruzzene M, Brunati AM, Cesaro L, Guerra B, et al. Different susceptibility of protein kinases to staurosporine inhibition. Kinetic studies and molecular bases for the resistance of protein kinase CK2. *Eur J Biochem* 1995;234(1):317–22.
- [25] Newton R, Bowler KA, Burns EM, Chapman PJ, Fairweather EE, Fritzl SJR, et al. The discovery of 2-substituted phenol quinazolines as potent RET kinase inhibitors with improved KDR selectivity. *Eur J Med Chem* 2016;112:20–32.
- [26] Nozal V, Martínez-González L, Gomez-Almeria M, Gonzalo-Consuegra C, Santana P, Chaikuad A, et al. TDP-43 Modulation by Tau-Tubulin Kinase 1 Inhibitors: a new avenue for future Amyotrophic Lateral Sclerosis Therapy. *J Med Chem* 2022;65(2):1585–607.
- [27] Nozal V, Martinez A. Tau Tubulin Kinase 1 (TTBK1), a new player in the fight against neurodegenerative diseases. *Eur J Med Chem* 2019;161:39–47.
- [28] Oliver JM, Burg DL, Wilson BS, McLaughlin JL, Geahlen RL. Inhibition of mast cell Fc epsilon R1-mediated signaling and effector function by the Syk-selective inhibitor, piceatannol. *J Biol Chem* 1994;269(47):29697–703.
- [29] Piotrowska H, Kucinska M, Murias M. Biological activity of piceatannol: leaving the shadow of resveratrol. *Mutat Res* 2012;750(1):60–82.
- [30] Roskoski R Jr. Properties of FDA-approved small molecule protein kinase inhibitors: a 2022 update. *Pharmacol Res* 2022;175:106037.
- [31] Rüegg UT, Burgess GM. Staurosporine, K-252 and UCN-01: potent but nonspecific inhibitors of protein kinases. *Trends Pharmacol Sci* 1989;10(6):218–20.
- [32] Sato S, Cerny RL, Buescher JL, Ikezu T. Tau-tubulin kinase 1 (TTBK1), a neuron-specific tau kinase candidate, is involved in tau phosphorylation and aggregation. *J Neurochem* 2006;98(5):1573–84.
- [33] Sato S, Xu J, Okuyama S, Martinez LB, Walsh SM, Jacobsen MT, et al. Spatial learning impairment, enhanced CDK5/p35 activity, and downregulation of NMDA receptor expression in transgenic mice expressing tau-tubulin kinase 1. *J Neurosci* 2008;28(53):14511–21.
- [34] Tamaoki T, Nomoto H, Takahashi I, Kato Y, Morimoto M, Tomita F. Staurosporine, a potent inhibitor of phospholipid/Ca⁺⁺-dependent protein kinase. *Biochem Biophys Res Commun* 1986;135(2):397–402.
- [35] Wang BH, Lu ZX, Polya GM. Inhibition of eukaryote serine/threonine-specific protein kinases by piceatannol. *Planta Med* 1998;64(3):195–9.
- [36] Wang Y, Mandelkow E. Tau in physiology and pathology. *Nat Rev Neurosci* 2016;17(1):5–21.
- [37] Xue Y, Wan PT, Hillertz P, Schweikart F, Zhao Y, Wissler L, et al. X-ray structural analysis of tau-tubulin kinase 1 and its interactions with small molecular inhibitors. *ChemMedChem* 2013;8(11):1846–54.
- [38] Yang EB, Zhao YN, Zhang K, Mack P. Daphnetin, one of coumarin derivatives, is a protein kinase inhibitor. *Biochem Biophys Res Commun* 1999;260(3):682–5.